Advances in Science and Technology Research Journal

*Advances in Science and Technology Research Journal*, 2025, 19(10), 359–370
https://doi.org/10.12913/22998624/207941
ISSN 2299-8624, License CC-BY 4.0

Received: 2025.05.05
Accepted: 2025.08.10
Published: 2025.09.01

# Designing an underwater towed vehicle using numerical methods

Radosław Kiciński[1*], Bogdan Szturomski[1], Andrzej Żak[1], Ryszard Studański[2]

[1] Mechanical Electrical Department, Polish Naval Academy, ul. Śmidowicza 69, 81-127 Gdynia, Poland
[2] Faculty Of Electrical Engineering, Gdynia Maritime University, ul. Morska 81-87, 81-225 Gdynia, Poland
* Corresponding author's e-mail: r.kicinski@amw.gdynia.pl

## ABSTRACT

The demand for energy resources, media, and information exchange in the 21st century is constantly growing. Numerous natural gas pipelines, power lines, telecommunications cables, and optical fibres are laid on the seabed. Additionally, offshore wind farms are being constructed in the Baltic Sea. Like any technical installation, these structures require regular supervision. In recent years, they have also become potential targets for terrorist attacks and acts of sabotage. Therefore, monitoring threats to critical underwater infrastructure has become increasingly important. This work presents the concept of an underwater towed vehicle designed for monitoring underwater installations. The proposed solution is relatively inexpensive and can be easily adapted to specific requirements and purposes. The study includes the proposed shape of the vehicle, methods for determining its dimensions, strength analysis using CAE software, and resistance and lift force calculations using CFD software. A simple propulsion and control system for the underwater thrusters is also proposed. The results of theoretical vehicle balancing calculations are presented as part of the concept verification.

**Keywords:** underwater towed vehicle, monitoring of underwater infrastructure, CAE, CFD.

## INTRODUCTION

The 21st century has expanded underwater infrastructure in the Baltic Sea. At the sea's bottom are optical fibres, power and telecommunications cables, and gas pipelines. This infrastructure requires constant control and supervision for operational and safety reasons. In recent years, critical infrastructure has become a target of terrorist attacks and hybrid wars [1]. For this reason, it is necessary, whenever possible, to monitor and identify potential threats continuously or systematically.

Moreover, the development of underwater robotics and environmental monitoring systems necessitated the need to provide wireless communication in water. In addition, there are the needs of the army and state services, e.g. in the field of minefield control or surveillance systems in strategic areas such as ports. Despite significant progress in developing telecommunications systems, wireless communication in the aquatic environment still poses many problems. Particular problems in obtaining relatively fast (in the order of kilobits) and reliable transmission are created by areas with intensive hydro technical development, such as ports, shallow water areas, and with variable sound wave propagation environments, e.g. in bottom sediments [2, 3].

Acoustic waves propagate best in an aquatic environment, so they are primarily used as a transmission medium. The propagation of sound waves in water is accompanied by many unfavourable phenomena that affect the overall quality of transmission expressed in terms of range, bit error rate, and speed. Among these phenomena, the most important are multipath, which leads to inter-symbol interference, selective fading in the frequency domain, and the Doppler effect [4–6].

Many commercial communication solutions used in deep waters do not work in a shallow

water area like the Baltic Sea, with variable salinity distribution as a function of depth and locally variable thermal conditions. Additionally, areas such as ports or canals, where the multiroute effect is very strong, most often completely exclude the possibility of using currently available equipment.

Therefore, we attempted to develop our own innovative solution for the underwater communication system, which, according to the assumptions, will resist selective frequency fading through collective reception. In 2022, project no. DOB-SZAFIR/01/B/017/04/2021 "Underwater wireless communication system for unmanned and autonomous maritime platforms" was obtained, the aim of which is to develop and build a demonstrator of an acoustic underwater communication system.

Concerning the project, this article also presented the methodology for designing such vehicles, considering their hydrodynamics and additional capabilities. The use of classic underwater vehicles may be ineffective due to their short range, limited autonomy and communication problems [7]. The solution to the abovementioned issues may be using underwater vehicles towed by a surface vessel. In this solution, the towed vehicle is only a carrier of measuring and monitoring equipment, which may be optical devices, echo sounders and any sensors, depending on the needs. The towed vehicle does not require a drive, complicated control or power sources, as it is possible to power the vehicle using a cable, which is also a tow rope. In practice, the measuring equipment constitutes the entire equipment of the towed vehicle, because the recording and processing of the received signals takes place on the towing unit. The vehicle does not require complicated control of its position, because the towing unit does this by sailing on an appropriate course, and the length of the towing rope regulates the immersion depth as a function of the towing speed. This solution is already used, among others, in towed sonars [8] and minesweepers [9]; however, it can be used for underwater monitoring or communications.

This approach generates many problems related to maintaining stability, trim and appropriate position behind the surface unit. As part of this work, it was decided to present and solve selected aspects of the design of towed vehicles using an underwater towed communication system as an example.

## PROBLEM DESCRIPTION

One of the project's key goals is to ensure wireless transmission underwater during the mutual movement of the transmitter and receiver. This necessitates moving sensors and electronic equipment underwater at relatively high speeds, i.e. up to 5 m/s. Therefore, it was decided to design a special housing enabling research and validation of the project assumptions. The housing design considers specific conditions important from the point of view of generating and receiving acoustic waves underwater under the assumed propagation conditions. Firstly, the communication system will be equipped with two transmitting hydrophones and four receiving hydrophones, which will ensure the possibility of collective reception and thus reduce phenomena related to the occurrence of selective fading. Secondly, the direct stream of water flowing around the hydrophones should not be affected. Locating the hydrophone outside the housing exposes it primarily to mechanical damage, and the direct impact of the flowing water on it, in particular the separation of the water stream and the possibility of cavitation, adversely affects the receiving properties of the hydrophone and may introduce interference in the recorded signal. Another requirement was to reduce the possibility of cavitation occurring on the casing. Cavitation bubbles occurring on the transmitter-receiver path make the propagation of the sound wave much more difficult, and usually completely prevent it. Due to the large difference in the density of two media, i.e. water and air, the acoustic wave at the border of these media is reflected and scattered. Therefore, there must be no cavitation interference along the length of the casing where the hydrophones are installed.

Moreover, the entire structure had to provide a tight place for the electronics necessary for the system's operation, which should be connected by cable to the computer on board the vessel. The structure is to be towed behind the ship using a signal cable that provides energy to the electronics in the underwater part and exchanges information between the communication module and the master computer located on the vessel. Using a binaural stocking, it was decided to make a mechanical connection between the housing and the cable. The correct operation of the system will be verified for various movement speeds; therefore, the stability of the movement of the entire structure

underwater, as well as the ability to adjust and, at least roughly, determine the vehicle's immersion depth, will be important during the tests.

Less essential requirements, but affecting the final form of the housing, were the lack of batteries or other heavy elements in the underwater part and, therefore, the impossibility of using them as ballast. Another aspect was the requirement for a relatively low weight of the entire structure to launch and lift it by a human or possibly by using a light crane. The above significantly impacts the arrangement of the centres of gravity and buoyancy in the vehicle and determines its final shape. The shape of the underwater vehicle's hull significantly impacts the hydrodynamic resistance [10] and the nature of the water flow, which translates into the towing force and the strength of the towing rope. An incorrect shape may cause cavitation to be generated within the hull, disrupting and hindering the measuring equipment's operation. The sources of cavitation are changes in shape, especially rapid changes in the radius of curvature. In the region of such geometry changes, local pressure drops to values at which the liquid boils can be expected. The optimal, proven shape is a section of pipe, the diameter and length of which depend on the equipment inside. The equipment of a towed vehicle usually requires placing it in an airtight container containing all the electronics. The tube is closed by the bow and stern, the primary purpose of which is to ensure the lowest possible resistance to movement and cavitation. Outside the hull, it is usually necessary to place depth controls, direction stabilisers and a towing handle, which disrupt the flow, so their location depends on the measurements being taken. The rudder setting can be constant or variable, controlled unattended or manually by the vehicle operator from the towing unit. Depending on the solution, a depth control setting mechanism is installed inside the hull in its aft part. Additionally, ballasts can be installed inside the vehicle to balance it properly.

It is assumed that the measuring equipment and most of the sensors are placed in a hermetic container or that the sensors are hermetic (to a given depth). Thus, the hull is an open structure flooded with water and does not have to meet the strength requirements due to the hydrostatic pressure of water, unlike an electronics container.

## METHODOLOGY OF THE DESIGN PROCESS

According to the described assumptions, such a vehicle should have low movement resistance. To minimise the drag force and limit the possibility of cavitation, making the bow and stern in several variants, such as semicircular and ellipsoidal shapes, tangentially connected to the cylindrical part, was proposed. This assumption was made based on the submarine design methodology [11–13]. Moreover, Defence Research and Development Canada (DRDC) has developed a typical hull for conventional ships and has repeatedly verified it with experimental tests [14]. The shape of the hull is described by appropriate equations and shown in Figure 1.

This model divides the ship into three sections: bow, circular middle and stern. It also assumes a basic slenderness factor of B/L = 8.75. In order to determine the exact values of the hull geometry, values must be calculated for each of the three elements:

- the bow part, whose shape is described by its function:

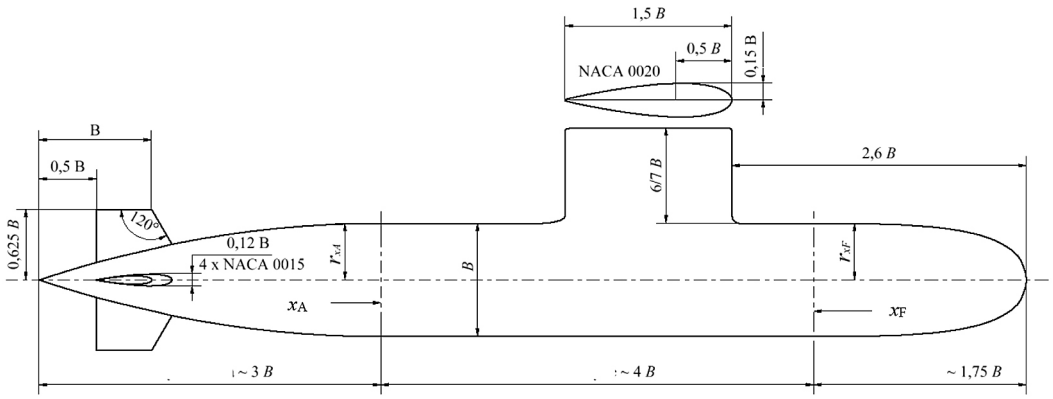


**Figure 1.** Profile of a standard submarine developed by DRDC

$$\frac{r_{xF}}{B} = 0.8685\sqrt{\frac{x_F}{B}} - 0.3978\frac{x_F}{B} + \\ + 0.006511\left(\frac{x_F}{B}\right)^2 + 0.005086\left(\frac{x_F}{B}\right)^3 \quad (1)$$

where: $r_{xf}$ is the radius of the section at a distance $x_F$ along the $x$ axis from the bow perpendicular, measured towards the stern, and $B$ is the hull diameter. The length of the bow part is equal to $1.75B$.

- midships (parallel middle body) of circular section with diameter $B$ having a length of four ship diameters ($4B$);
- the stern part has a length equal to three ship diameters ($3B$). The shape of the stern part of the ship is described by the relationship.

$$\frac{r_{x_A}}{B} = \frac{1}{3}\left(\frac{x_A}{B}\right) - \frac{1}{18}\left(\frac{x_A}{B}\right)^2 \quad (2)$$

where: $r_{xA}$ – the radius of the section at the distance $x_A$ along the $x$ axis from the stern, measured towards the bow.

The presented model refers to a submarine, but the bow and stern shape can be successfully used to design underwater towed vehicles. The shape of the bow and stern proposed for the towed vehicle is shown in Figure 2.

The length and diameter of the central part depend on the vehicle equipment. In the case of an underwater communication vehicle, it is important to arrange the hydrophones in a sufficiently large space, so the length of the working part is approximately 20 times its diameter. According to the description, the underwater towed vehicle should be equipped with rudder fins. As part of this solution, a dynamic immersion system was proposed, made of flat panels and their adjustment mechanism. The entire system is hidden inside the stern part (Figure 3).

The vehicle is affected by gravity forces from all equipment elements, the weight of the hull, mountings, etc., which can be reduced to one point called the centre of gravity (COG). This point is acted upon by the resultant force of

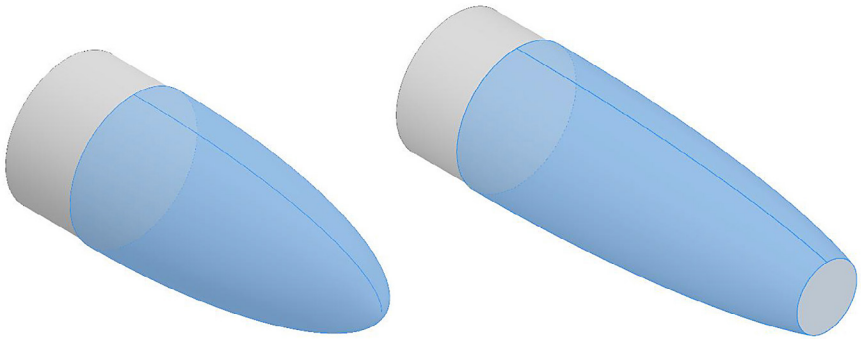

**Figure 2.** The shape of the bow and stern complies with DRDC guidelines

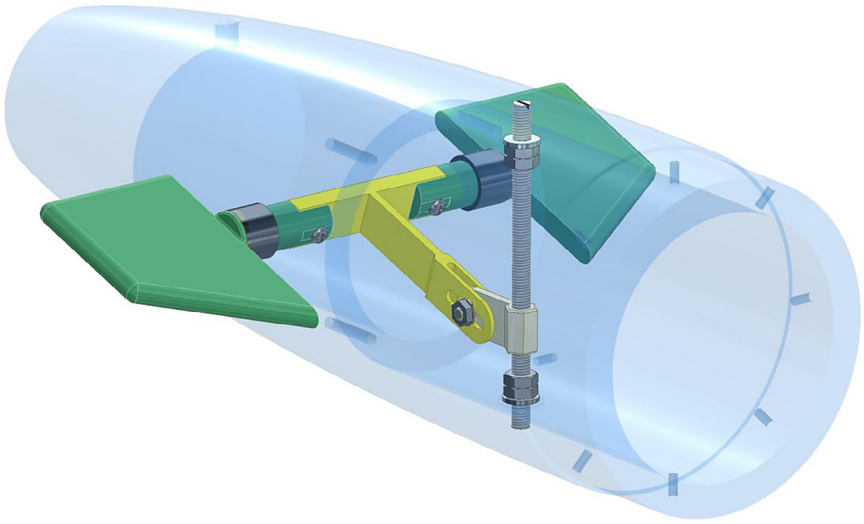

**Figure 3.** The rudder mechanism, which is mounted in the stern underwater part of the towed vehicle

gravity directed vertically downwards, marked as $F_g$. The pressure forces of the surrounding water act upon the outer, submerged, watertight part of the hull. According to the law of pressure propagation in fluids, the vehicle will be pressurised on all sides. The pressure forces will be directed perpendicular to the curvature of the hull and proportional to the depth at which the underwater vehicle is located. If the hull surfaces are divided into identical elementary planes, then a force perpendicular to each plane will act. These forces can be divided into vertically and horizontally directed components. By dividing the hull with a plane of symmetry, it can be seen that the horizontal components become zero and the vertical components form the resultant. The sum of the components of vertical forces directed downwards is always smaller than those directed upwards. Therefore, the resultant of the buoyancy force, marked as $F_w$, will be directed upwards and applied at the centre of gravity of the submerged volume of the ship COB (centre of buoyancy) (Figure 4).

The value of the buoyancy force depends on the volume of the immersed part of the hull $V$ and the specific gravity of water $\gamma$, therefore

$$F_w = V\gamma \tag{3}$$

As the above considerations show, gravity and buoyancy forces affect the vehicle suspended in the water. If the weight of the ship is equal to the buoyant force, then the vessel is in equilibrium, so

$$V\gamma = mg \tag{4}$$

where: $V$ – volume of the immersed part of the hull, m$^3$; $\gamma$ – specific gravity of water, N/m$^3$; m – vehicle mass, kg; $g$ – acceleration of gravity, m/s$^2$.

In order to keep the vehicle on an even keel (zero trim and heel), the points of application of gravity and buoyancy forces should be in one line:

$$\begin{aligned} x_{COB} &= x_{COG} \\ y_{COB} &= y_{COG} \end{aligned} \tag{5}$$

In the case of a towed vehicle with a symmetrical circular cross-section, the centres of buoyancy and gravity are not at the same point, which causes an imbalance in the underwater position. The presented vehicle is also unbalanced in terms of trim, so it should be equipped with a ballasting system. Nowadays, such a system can be made as a constant or variable ballast using water, compressed air or built-in variable volumes such as pistons with a cylinder or buoyancy balloons. In the presented project, it was decided to place movable permanent ballasts mounted in the bow and stern parts. Placing the ballast below the centre of buoyancy is essential to lower the centre of gravity and increase vehicle stability. The initial vehicle geometry is shown in Figure 5.

The next stage was to determine the centers of gravity and buoyancy for the presented project. For this purpose, the CAD (computer aided design) environment was used. The center of gravity was determined using the basic tools of the program, while to determine the center of buoyancy it was necessary to fill the empty space for

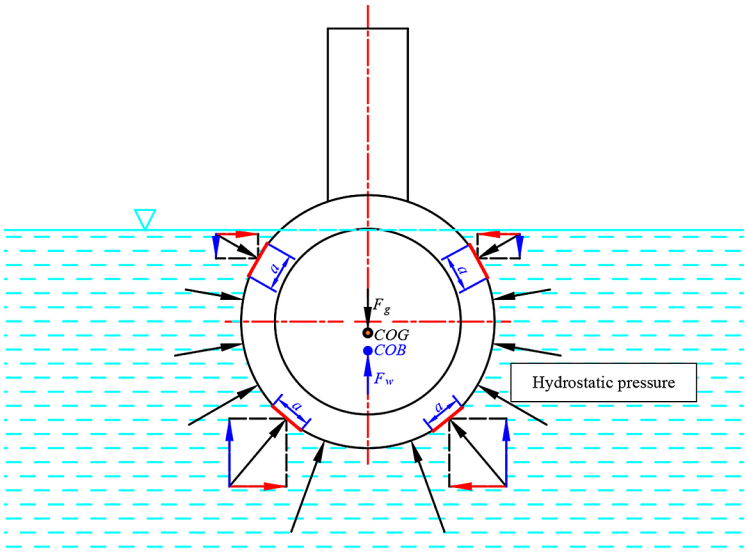


**Figure 4.** Illustration of the buoyancy force and the hydrostatic pressure load on the hull

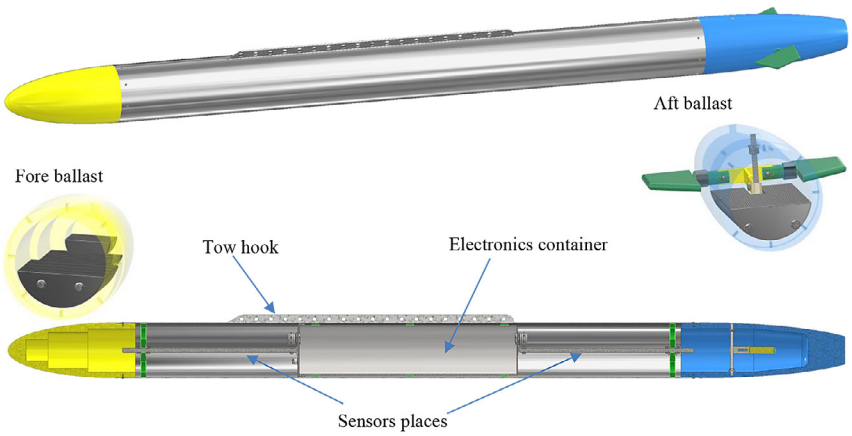


**Figure 5.** Preliminary design of a towed vehicle

electronics and determine the center of buoyancy using the same tools. The buoyancy force determined on the basis of geometric parameters obtained from the CAD program is:

$$W = V_z \rho_w g = 0.01866 \cdot 1000 \cdot 9.81 = 183.05 \text{ N}$$

and the weight accordingly:

$$G = M_c g = 35.032 \cdot 9.81 = 343.66 \text{ N}$$

So the difference is:

$$F_R = G - W = 343.66 - 183.05 = 160.61 \text{ N}$$

where: $W$ – buoyant force, N; $G$ – gravity force, N.

The coordinates of the centre of buoyancy are: $x_w = 1113.7$ mm, $y_w = -4.5$ mm, $z_w = 0.0$ mm. The coordinates of the centre of gravity are: $x_G = 1148.9$ mm, $y_G = -11.8$ mm, $z_G = 0.0$ mm. So: $\Delta x = 35.2$ mm, $\Delta y = 7.3$ mm.

The difference between the centre of buoyancy and gravity is only 7.3 mm. This may not be sufficient for the stable movement of the probe during towing. For this reason, an alternative solution was proposed to load the probe with an additional streamlined ballast weighing 1.047 kg. This solution allows you to install ballast of any weight depending on your needs. It will slightly increase the flow resistance but will lower the centre of gravity and, at the same time, reduce the stern ballast, which will shift the centre of gravity towards the bow and reduce the weight of the entire structure. This is advantageous for a towed probe. In such a case, the centre of gravity should be between the centre of buoyancy and the point of application of the towing force. The geometric parameters for the probe with an additional streamlined ballast weighing 1 kg are (Figure 6):

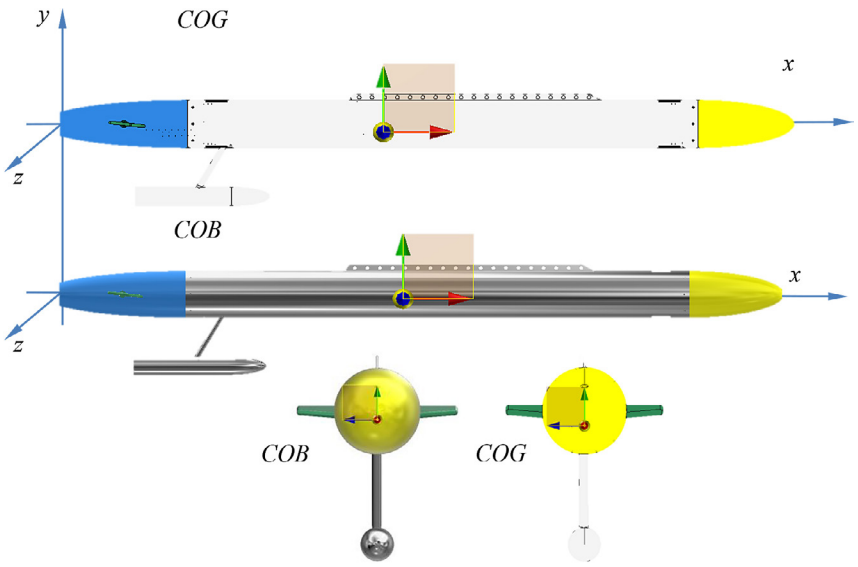


**Figure 6.** Coordinates of the centre of buoyancy and gravity of the vehicle with keel and ballast

$$W = V_z \rho_w g = 0.01803 \cdot 1000 \cdot 9.81 = 176.87 \text{ N}$$

$$G = M_c g = 30.056 \cdot 9.81 = 294.85 \text{ N}$$

$$F_R = G - W = 294.85 - 176.87 = 117.98 \text{ N}$$

The coordinates of the centre of buoyancy are: $x_w$ = 1149.4 mm, $y_w$ = – 5.6 mm, $z_w$ = 0.0 mm. The coordinates of the centre of gravity are: $x_G$ = 1278.8 mm, $y_G$ = – 18.1 mm, $z_G$ = 0.0 mm. So: $\Delta x$ = 129.4 mm, $\Delta y$ = 12.5 mm.

## HYDRODYNAMIC BALANCE

Knowing the places where static forces were applied, the vehicle's dynamics had to be determined. While moving, the hull of the towed underwater vehicle is also affected by the lifting force from the rudders, the lifting force from the hull, the drag force, and the force from the towing rope. When considering the vehicle's balance during towing, it is most reasonable to adopt the coordinate system at the rope attachment point (Figure 7).

Balance equations of the probe with respect to the adopted coordinate system:

$$\sum F_{ix} = -S_x - R_x + F_x = 0 \tag{6}$$

$$\sum F_{iy} = S_y + R_y + W - G + F_y = 0 \tag{7}$$

$$\sum M_{iz} = -S_y \cdot x_S - S_x \cdot y_S - R_x \cdot y_R - R_y \cdot x_R - W \cdot x_W + G \cdot x_G = 0 \tag{8}$$

Then the towing force is:

$$F_y = -S_y - R_y - W + G \tag{9}$$

$$F_x = S_x + R_x \tag{10}$$

$$F = \sqrt{(-S_y - R_y - W + G)^2 + (S_x + R_x)^2} \tag{11}$$

The angle of inclination of the tow rope expressed in degrees is:

$$\arctan \alpha = \frac{-S_y - R_y - W + G}{S_x + R_x} \cdot \frac{\pi}{180} \tag{12}$$

Analysing the above equations, it can be seen that the unknowns are the drag forces and the forces on the rudders. In order to dynamically balance the vehicle, these values should be initially determined using analytical equations and CFD analyses [20]. According to the theory of fluid mechanics, the resistance of a body immersed in a liquid depends on the square of the swimming speed and specific constant values presented in the form

$$R = c_f \cdot \frac{\rho v^2}{2} \cdot A \tag{13}$$

where: $R$ – drag, N; $c_f$ – drag coefficient; $\rho$ – water density, kg/m$^3$ ($\rho$ = 1025 kg/m$^3$); $v$ – velocity, m/s (1 w = 0.5145 m/s); $A$ – hull wetted surface, m$^2$.

The resistance of a body in water can be divided into the resistance of the bare hull and the resistance of parts that are difficult or sometimes impossible to model in calculations or in model tests. These include, among others, supports, covers, propellers, splitters, etc. The total water drag to the vehicle will be equal to the sum of the drags listed below

$$R = R_t + R_{prot} + R_{wave} \tag{14}$$

where: $R_t$ – friction drag, $R_{prot}$ – protruding parts drag, $R_{wave}$ – wave drag.

In the case under consideration, only the resistance of protruding parts and friction resistance are taken into account for an underwater vehicle.

A body in motion encounters the intermolecular forces of the water surrounding it, called frictional drag. In order to determine the frictional drag coefficient, the Reynolds number must be

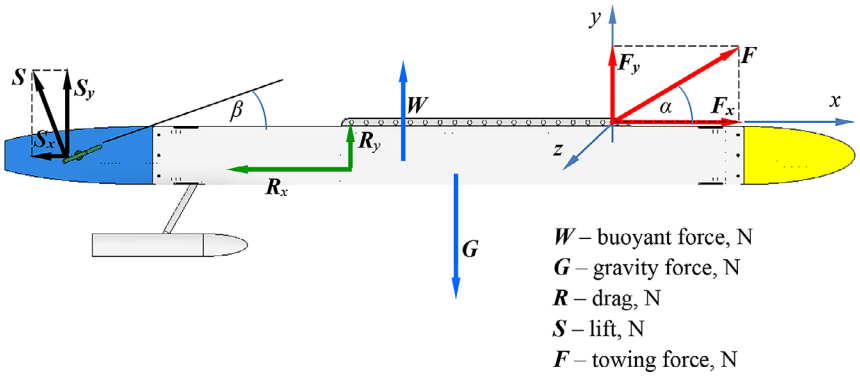


**Figure 7.** Distribution of forces acting on a towed underwater vehicle

defined. This number allows you to estimate the ratio of active forces to passive forces (inertia forces) occurring during fluid movement, related to internal friction in the fluid, which manifests itself in the form of viscosity. The Reynolds number is determined as:

$$Re = \frac{v \cdot L}{\nu} \tag{15}$$

where: $v$ – velocity, m/s; $L$ – characteristic length, in the case under consideration, the length of the vehicle, m; $\nu$ – kinematic viscosity, m$^2$/s.

Based on model tests, a number of formulas were developed to determine the frictional resistance coefficient of a flat plate $c_f$ as a function of the Reynolds number, and so [15]:

- from the Prandtl-Schlichting formula

$$c_{f0} = 0.455[\log_{10} \cdot Re]^{-2.58} \tag{16}$$

- from the ITTC formula

$$c_{f0} = \frac{0.075}{(\log Re - 2)^2} \tag{17}$$

The next step necessary to determine the drag characteristics is to determine the hull's wetted surface. This surface is directly immersed in the liquid, and the friction force acts on it.

Computer techniques were used to calculate the wetted area of the entire hull. Based on the model made in CAD, the wetted surface of the vehicle was calculated as $A$ = 1.33 m$^2$. It is therefore possible to analytically determine the vehicle drag using the above relationships:

- Reynolds number for 5 m/s

$$Re = \frac{5 \cdot 2.3}{10^{-6}} = 11.5 \cdot 10^5$$

- frictional drag according to the Prandtl-Schlichting formula

$$R = 0.0044 \cdot \frac{1025 \cdot 5^2}{2} \cdot 1.33 = 72.19 \text{ N}$$

- frictional drag according to the ITTC formula

$$R = 0.0045 \cdot \frac{1025 \cdot 5^2}{2} \cdot 1.33 = 75.37 \text{ N}$$

Analytical calculations refer to simple cases and do not take into account protruding parts and other resistance components. Therefore, additional CFD simulations were performed to compare the calculations.

The simulations were performed in a steady state, with an iterative change of the flow speed from 1 to 5 m/s. The turbulence properties were then determined based on the Reynolds number. The Reynolds number indicates that this is a turbulent flow and, as such, requires additional modelling. There are many models, but practice shows that the k-ω SST model works best for streamflows *k-ω* SST [16]. The *k-ω* SST (Shear-Stress Transport) model is one of the more advanced and popular variants of the k-ω model in the field of CFD. It combines the advantages of the *k-ω* and *k-ε* models to obtain more accurate results under various flow conditions.

The *k-ω* SST model distinguishes two areas:

- boundary region – in the boundary layer, the model behaves as *k-ω*, which allows accurate accounting of the boundary layer and related phenomena such as boundary layer movement.
- free region – in the free area, the model switches to *k-ε* behaviour, which accounts for the interaction between large and small turbulent scales.

Using this approach, the *k-ω* SST model is effective both in near-wall conditions, where the boundary layer is important and in free regions, where turbulence is the dominant factor. This makes it often chosen for flow simulation in various applications such as hydrodynamics, aerospace and hydraulics.

The results of CFD calculations determine the drag force at the level of 88 N, so they are consistent with analytical calculations. It follows that the resistance of the protruding parts is approximately 20% of the total resistance, which is consistent with the literature [11, 17]. The calculations were performed for a mesh of tetragonal elements. The task consisted of 4810163 nodes and 23940237 elements. The velocity distribution and the mesh view around the probe with the optimised shape are shown in Figure 8.

After conducting the simulation, the vehicle resistance forces were determined as a function of the towing speed. After calculations, the drag of the vehicle can be described by the equation:

$$R = 3v^2 + 2.65v \tag{18}$$

After determining the model's compliance with the analytical calculations, an analysis of the forces acting on the vehicle hull, depending on the angle of attack of the stern rudders, was carried out, following methodologies applied previously in aerodynamic analyses of stabilizer control surfaces [22]. Please note that the rudder is not the only supporting surface of the vehicle.

Lifting force is also generated by its hull, depending on its angle in relation to the towing force, and all protruding elements.

The Table 1 presents the results of the drag force, the lift force on the rudders, and the lift force generated by the entire probe body (lift total). Research on real objects shows that the drag force is approximately 20% higher than the results obtained in CFD simulations [18–21]. So for a speed of 5 m/s, it will be approximately 110 ÷ 120 N.

Knowing the values of the forces on the controls and the drag forces, the vehicle's dynamic balancing can be determined (Figure 9). For an underwater vehicle towed at a speed of 5 m/s with a ballast keel and ballasts at the bow, the force values and their coordinates are listed in Table 1. In order for the probe not to rotate around the rope hook and to move vertically in the water, the total torque must be close to zero, and for the above data, it is 21.3 Nm. To balance the moment of force causing the vehicle to rotate, the depth controls at the stern should be deflected to generate a moment of force of a value close to 21.3 Nm. This value will be obtained for the lift force of the rudders equal to 13 N, then the optimal solution will be obtained (Table 2).

$$F_v = -13.0 - 10 - 176.9 + 294.9 = -95 \text{ N}$$

$$F_x = -125 \text{ N}$$

$$\sum M_{iz} = 13 \cdot 1638 + 125 \cdot 99 + 10 \cdot 938 + 176.9 \cdot 688.7 - 294.9 \cdot 559.2 = 0.02 \text{ Nm}$$

$$F = \sqrt{125^2 + 95^2} = 157 \text{ N}$$

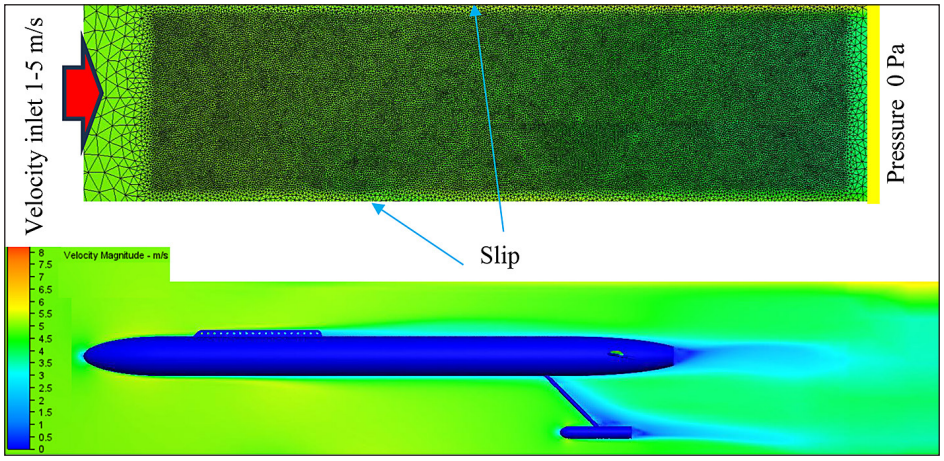


**Figure 8.** Water velocity distribution around the towed vehicle and simulation boundary conditions

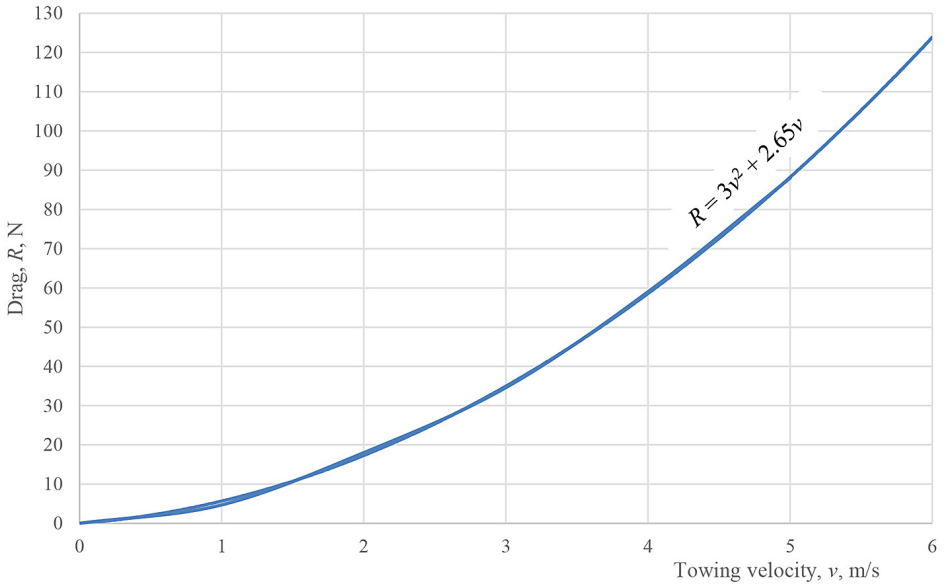


**Figure 9.** Vehicle drag characteristics

**Table 1.** Values of forces acting on the vehicle hull and rudders - results of CFD calculations

| | | $v$, m/s | | | | | |
|---|---|---|---|---|---|---|---|
| Angle $\beta$ | | 0 | 1 | 2 | 3 | 4 | 5 |
| -5 | $R$ | 0 | 4.5 | 16.5 | 33.8 | 57.8 | 86 |
| | $S_y$ | 0 | -0.8 | -4 | -10 | -18.4 | -28 |
| | Lift total | 0 | -1.3 | -6 | -14.7 | -27.4 | -43 |
| -3 | $R$ | 0 | 4.5 | 17 | 33.3 | 56 | 84 |
| | $S_y$ | 0 | -0.5 | -3 | -6 | -10.6 | -17 |
| | Lift total | 0 | -0.8 | -4 | -8 | -14.5 | -23 |
| -2 | $R$ | 0 | 4.5 | 16.7 | 33 | 56 | 86 |
| | $S_y$ | 0 | -0.2 | -1.8 | -3.8 | -7.2 | -13.4 |
| | Lift total | 0 | -0.5 | -2.5 | -5 | -9.7 | -17 |
| 0 | $R$ | 0 | 4.7 | 18 | 34.6 | 59 | 88 |
| | $S_y$ | 0 | 0 | 0 | 0 | 0.06 | -1 |
| | Lift total | 0 | 0.5 | 1 | 1.8 | 3.1 | 4.8 |
| 2 | $R$ | 0 | 4.5 | 16 | 33.5 | 55.5 | 84 |
| | $S_y$ | 0 | 0.5 | 1.8 | 4.6 | 8 | 12 |
| | Lift total | 0 | 0.7 | 3.5 | 9.4 | 16 | 25.5 |
| 3 | $R$ | 0 | 4.3 | 16.4 | 33.5 | 57 | 85 |
| | $S_y$ | 0 | 0.5 | 2.7 | 6.6 | 12 | 18.7 |
| | Lift total | 0 | 0.96 | 5 | 12 | 22 | 35 |
| 5 | $R$ | 0 | 4.7 | 16.7 | 33.7 | 56.8 | 87 |
| | $S_y$ | 0 | 1 | 4.5 | 10.6 | 17.2 | 29.2 |
| | Lift total | 0 | 1.9 | 7.8 | 18.8 | 32.6 | 54 |

**Table 2.** Force values and their coordinates (coordinate system in hook No. 1)

| | Force value, N | Force value, N | $x$ mm | $y$ mm | Moment of force $M_z$, Nm |
|---|---|---|---|---|---|
| Buoyancy force $W_y$ | | 176.9 | -688.7 | -94.6 | -121.8 |
| Gravity force $G_y$ | | -294.9 | -559.2 | -107.1 | 164.9 |
| Drag $R_x$ | -125 | | -938 | -99 | 12.4 |
| Drag $R_y$ | | 10 | -938 | -99 | -9.4 |
| Control surface drag $S_x$ | 0 | | -1638 | -89 | 0.0 |
| Control surface lift $S_y$ | | 13 | -1638 | -89 | 0.0 |
| Towing force $F$ | -125 | -95 | $\sum M_{iz}$ | | 0.02 |

$$\arctan\alpha = \frac{95}{125}\cdot\frac{\pi}{180} = 37.2°$$

For this case, the towing force in the tow rope is 157 N, acting at an angle of 37.2°. The calculations performed are illustrative because, at this stage of the project, there is no information about the electronics chamber's equipment and the sensors' shape and weight. Moreover, the values of the resistance force are obtained as a result of CFD calculations, which must be verified experimentally on a measurement station designed for this purpose. Based on the presented methodology, a towed vehicle was made and has been subjected to experimental tests (Figure 10).

Experimental tests were conducted at the Ship Design and Research Centre (CTO S.A.) in a towing tank with dimensions of 260 × 12 × 6 m, equipped with a movable carriage capable of reaching speeds up to 12 m/s. Initial static submersion tests confirmed the correct selection of mass distribution and the proper positioning of the centre of gravity and the centre of buoyancy.

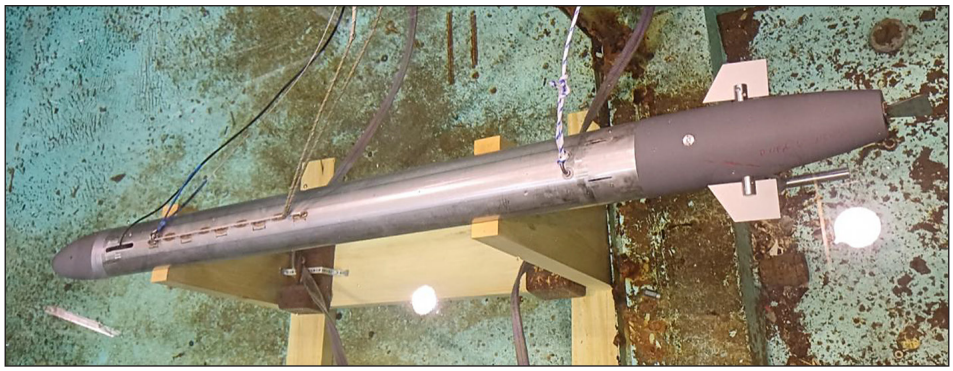

**Figure 10.** Towed underwater vehicle prepared for model tests

The vehicle exhibited stable behaviour during water entry and consistently returned to its upright position after being tilted.

In the next phase, the vehicle was towed at various speeds to evaluate its dynamic trim and investigate the potential occurrence of cavitation. No cavitation was observed at speeds up to 5 m/s. However, at speeds exceeding 4 m/s, the vehicle showed a tendency to rise toward the surface due to lift forces generated along the hull. This behaviour necessitated dynamic trim corrections, which were implemented by adjusting the deflection angle of the stern control surfaces.

After applying these modifications, the vehicle demonstrated hydrodynamic behaviour in line with the design assumptions.

## CONCLUSIONS

The presented study developed a comprehensive methodology for designing underwater towed vehicles dedicated to monitoring underwater infrastructure, with particular emphasis on hydrodynamic conditions in shallow waters, such as the Baltic Sea. The project effectively combined classical engineering approaches from fluid mechanics with modern numerical methods (CAE and CFD), enabling precise shaping of the vehicle's geometry to minimize hydrodynamic drag and reduce cavitation risk.

The proposed vehicle design, based on submarine hull solutions (e.g., DRDC standard), proved effective both in numerical simulations and experimental model tests. CFD simulations using the k-ω SST turbulence model confirmed that the ellipsoidal bow and stern shapes significantly reduce drag and eliminate cavitation at speeds up to 5 m/s. The total hydrodynamic drag of the fully equipped probe was determined to be approximately 90 N in CFD simulations, with real drag expected to be around 110–120 N, which aligns with known tolerances in hydrodynamic analyses (~20%).

A key contribution of this work is the development of a simplified yet effective analytical and numerical balancing methodology for forces acting on the towed vehicle. This ensures stable vehicle behavior during towing operations at speeds up to 5 m/s. The mechanical depth control system, based on manually adjustable stern fins and supplemented with a keel-mounted ballast, provided sufficient static and dynamic balance during experimental tests. This approach eliminates the need for complex onboard systems, aligning with the goal of creating simple and reliable platforms for critical infrastructure monitoring.

The project also demonstrated the feasibility of integrating the towed vehicle concept with underwater acoustic communication systems, offering a promising platform for future applications in reconnaissance, environmental monitoring, and military operations. Compared to self-propelled underwater vehicles, the towed solution is simpler, lighter, and offers longer operational ranges without the limitations imposed by onboard power supplies.

Future developments should focus on introducing active depth control systems, automatic ballast adjustments, and adaptive control of steering surfaces based on sensor feedback. Additionally, integration with modern underwater communication technologies, such as adaptive algorithms and MIMO systems, could further enhance the operational capabilities of such platforms.

Finally, it should be emphasized that while numerical methods such as CFD provide valuable

insights, they must be verified through physical model tests in controlled environments, as performed in this study, in accordance with best practices established in aerodynamic research of hybrid platforms.

The proposed methodology represents a practical, systematic, and verifiable engineering approach to designing underwater towed vehicles for use in challenging marine environments.

## REFERENCES


1. Sanderson H, Czub M, Koschinski S, Tougaard J, Sveegaard S, Jakacki J, et al. Environmental impact of sabotage of the Nord Stream pipelines. In Review; 2023. https://doi.org/10.21203/rs.3.rs-2564820/v1
2. Stojanovic M, Catipovic J, Proakis JG. Adaptive multichannel combining and equalization for underwater acoustic communications. The Journal of the Acoustical Society of America 1993;94:1621–31. https://doi.org/10.1121/1.408135
3. Kochanska I. Reliable OFDM data transmission with pilot tones and error-correction coding in shallow underwater acoustic channel. Applied Sciences 2020;10:2173. https://doi.org/10.3390/app10062173
4. Ganesh P S S P, Venkataraman H. E-CRUSE: Energy-based Throughput analysis for cluster-based RF shallow underwater communication. IET Communications 2020;14. https://doi.org/10.1049/iet-com.2019.1294
5. Zhu S, Chen X, Liu X, Zhang G, Tian P. Recent progress in and perspectives of underwater wireless optical communication. Progress in Quantum Electronics 2020;73:100274. https://doi.org/10.1016/j.pquantelec.2020.100274
6. Czapiewska A, Łuksza A, Studański R, Wojewódka Ł, Żak A. Comparison of doppler effect estimation methods for MFSK transmission in multipath hydroacoustic channel. IEEE Access 2024;12:49976–86. https://doi.org/10.1109/ACCESS.2024.3385441
7. Łarzewski B, Hałas J, Powarzyński D, Lewandowski J, Piskur P. Design and implementation of an unmanned underwater vehicle with hybrid drive – REBA. PAR 2022;26:61–7. https://doi.org/10.14313/PAR_246/61
8. Stema Systems. Klein 5000. Stema Systems 2024. https://stema-systems.nl/equipment/klein-5000/ (accessed June 10, 2024).
9. ZBIAM. Demonstrator trału niekontaktowego MLM II z OBR CTM S.A. Wydawnictwo militarne ZBIAM 2020. https://zbiam.pl/demonstrator-traluniekontaktowego-mlm-ii-z-obr-ctm-s-a/ (accessed June 10, 2024).
10. Renilson M. Submarine Hydrodynamics. Cham: Springer International Publishing; 2018. https://doi.org/10.1007/978-3-319-79057-2_1
11. Polish DoD. Teoria okrętów podwodnych [Submarine Theory - in Polish]. Gdynia: Polish DoD; 1965.
12. Gabler U. Submarine design. Koblenz: Bernard & Graefe; 1986.
13. Suh S-B, Park I-R. Numerical Simulation of the Flow Around the SUBOFF Submarine Model Using a DES Method. JSNAK 2021;58:73–83. https://doi.org/10.3744/SNAK.2021.58.2.073
14. Michael M, Atlantic DRC-. The Standard Submarine Model: a Survey of Static Hydrodynamic Experiments and Semiempirical Predictions. Defence R&D Canada - Atlantic; 2003.
15. Kiciński R, Jurczak W. Submarine resistance force characteristics determination after modification of depth rudder system. Adv Sci Technol Res J 2021;15:1–9. https://doi.org/10.12913/22998624/125186
16. Pawłucki M, Kryś M. CFD dla inżynierów. Praktyczne ćwiczenia na przykładzie systemu ANSYS Fluent. 2021.
17. Charchalis A. Opory okrętów wojennych i pędniki okrętowe (Resistance force of warships and ship propellers - in Polish). Gdynia: Akademia Marynarki Wojennej im. Bohaterów Westerplatte; 2001.
18. Quang HL. Best Practice Guidelines for Marine Applications of Computational Fluid Dynamics 2003.
19. Malinowska K. Porównanie komputerowych metod obliczania oporu jednostki żaglowej z metodą doświadczalną. Prace Wydziału Nawigacyjnego Akademii Morskiej w Gdyni 2017;Z. 32. https://doi.org/10.12716/1002.32.04
20. Czyż Z, Karpiński P, Skiba K, Bartkowski S. Numerical calculations of water drop with a firefighting plane. Applied Computer Science. 2023;19(3):19–20.
21. Czyż Z, Karpiński P, Skiba K., Wendeker M. Measurements of aerodynamic performance of a hybrid multirotor fuselage with autorotation capability. International Review of Aerospace Engineering (IREASE). 2022;15(1):12–23. https://doi.org/10.15866/irease.v15i1.21319
22. Czyż Z, Karpiński P. Aerodynamic characteristics of the x-tail stabilizer of a hybrid unmanned aircraft. International Journal of Simulation Modelling (IJSIMM). 2020;19(4):631–642.